Legacy effects of sorption determine the formation efficiency of mineral-associated soil organic matter

Shuling Chen[1,2,*], Thimo Klotzbücher[2], Oliver J. Lechtenfeld[3], Hanlie Hong[4], Chongxuan Liu[1], Klaus Kaiser[2], Christian Mikutta[5], Robert Mikutta[2]

[1] China State Environmental Protection Key Laboratory of Integrated Surface Water-Groundwater Pollution Control, School of Environmental Science and Engineering, Southern University of Science and Technology, 518055 Shenzhen, China

[2] Soil Science and Soil Protection, Martin Luther University Halle-Wittenberg, Von-Seckendorff-Platz 3, 06120 Halle (Saale), Germany

[3] Department of Analytical Chemistry, Research group BioGeoOmics, Helmholtz Centre for Environmental Research-UFZ, Permoserstraße 15, 04318 Leipzig, Germany

[4] State Key Laboratory of Biogeology and Environmental Geology, China University of Geosciences, 430074 Wuhan, China

[5] Institute of Mineralogy, Faculty of Natural Sciences, Gottfried Wilhelm Leibniz University Hannover, Callinstrstraße 3, 30167 Hannover, Germany

***** Corresponding author：slchen@cug.edu.cn

ABSTRACT: Sorption of dissolved organic matter (DOM) is one major pathway in the formation of mineral associated-organic matter (MOM) but there is little information how previous sorption events feedback to later ones by leaving their imprint on mineral surfaces and solutions (`legacy effect`). In order to conceptualize the role of legacy effects in MOM formation, we conducted sequential sorption experiments with kaolinite and gibbsite as minerals and DOM derived from forest floor material. The MOM formation efficiency leveled off upon repeated addition of identical DOM solutions to minerals due to the retention of highly sorptive organic molecules (primarily aromatic, nitrogen-poor, hydrogen-poor, and oxygen-rich molecules), which decreased sorption site availability and simultaneously modified mineral surface charge. Organic-organic interactions as postulated in multilayer models played a negligible role in MOM formation. Continued exchange between DOM and MOM molecules upon repeated sorption altered DOM composition but not MOM formation efficiencies. Sorption-induced depletion of high-affinity compounds from solutions further decreased MOM formation efficiencies to pristine minerals. Overall, the interplay between the differential sorptivities of DOM components and mineral surface chemistry explains legacy effects that contribute to the regulation of fluxes and distribution of organic matter in soil.

KEYWORDS: *soil organic matter, mineral-associated organic matter, sorption, carbon sequestration, Fourier-transform ion cyclotron resonance mass spectrometry, legacy effects*

SYNOPSIS: Our work informs on mechanisms in the formation of mineral-associated organic matter relevant for explaining site-dependent differences in the build-up of stable soil organic matter and developing strategies that aim at increasing soil carbon.

INTRODUCTION

Enhancing soil organic matter (OM) levels is widely considered a main aim of strategies mitigating global challenges such as climate change and ecosystem degradation.[1] Soil mineralogy is a main factor of OM accumulation during soil development[2,3] as the sorption of organic molecules to surfaces of soil minerals decreases their bioavailability and turnover time.[4,5] The efficiency of MOM formation, i.e., how much of OM input to soil is transferred to MOM, has thus been proposed as key determinant of the carbon (C) balance of ecosystems.[6] Yet, pathways and efficiencies of MOM formation under variable soil conditions are still not well understood and conceptualized.[7,8] Dissolved organic matter (DOM) released during the decay of plant litter or recycling of microbial bio- and necromass presumably is the major source of MOM.[9-13] Laboratory sorption experiments conducted under a wide range of conditions provided insight into a variety of chemical mechanisms by which DOM components bind to mineral surfaces.[4] They mostly were conducted using pristine mineral surfaces, while in soil DOM typically interacts with mineral surfaces already coated with OM. Proposed soil OM concepts are contradictory regarding the question on how continuous input of DOM interacts with MOM formation. The concept of C saturation presumes a maximum amount of OM that can be stored in soil.[14,15] Accordingly, growth of MOM coatings on mineral surfaces may also be limited and reach saturation levels.[7,8,16] On the other hand, MOM coatings may promote DOM sorption by organic-organic interactions,[17-20] as presumed in the `multilayer` model of MOM.[21,22] These considerations demonstrate that we need to better understand how legacy effects induced by sorption processes shape MOM formation in soil quantitatively and qualitatively, meaning that chemical alterations at mineral surfaces induced by former sorption events may affect MOM formation at later ones.

A second type of legacy effect driving MOM formation efficiencies might be due to sorptive alterations of soil solutions. Typically, sorption events selectively remove organic components from solution, which simultaneously reduces concentrations and alters the composition of DOM. Sorptive fractionation generally suggests variable affinities of DOM components to sorb to minerals,[23] which in turn may alter the sorptivity of the remaining DOM during later sorption events. Assessing these interactions across `sequences` of sorption events is, for instance, critical for understanding the distribution of OM and efficiencies of MOM formation in whole soil profiles under humid climate, where soil solution chemistry is continuously altered by sorption processes during percolation through soil profiles.[10,24,25]

Taken together, sorption events shape the chemistry of soil environments by simultaneously altering mineral surface properties and solutions. These alterations may feedback on subsequent sorption events, and ultimately determine element cycling in soil. We aimed at quantifying and elucidating the mechanisms by which legacy effects modulate the efficiency of MOM formation. To this end, we conducted a laboratory sorption experiment, consisting of two treatments (Figure 1). In the first treatment, we repeatedly added identical fresh DOM solutions (DOM_{fresh}) to minerals to assess the gradual formation of OM coatings and the efficiency of MOM formation. In the second treatment, we applied the reacted solutions (DOM_{react}) from the first treatment to a second set of initially pristine minerals in order to assess the effects of changes in solution chemistry due to previous sorption events on subsequent MOM formation.

We hypothesized that MOM formation continues upon repeated DOM additions with only minor decreases in efficiencies as, according to multilayer models, MOM formation might continue via organic-organic interactions. Thus, the dominant mechanisms of MOM formation were expected to change upon repeated DOM additions (with organic-organic interactions becoming increasingly

92 important), mirrored by sorptive fractionation patterns of DOM. We expected that the initial
93 properties of minerals (gibbsite vs. kaolinite) determine MOM formation efficiencies at the first
94 DOM addition, while the influence should decrease at repeated DOM addition when organic-
95 organic interactions dominate. We further hypothesized that sorptive alterations of DOM due to
96 preferential loss of the most sorptive components greatly reduce efficiencies of MOM formation
97 in subsequent sorption events.

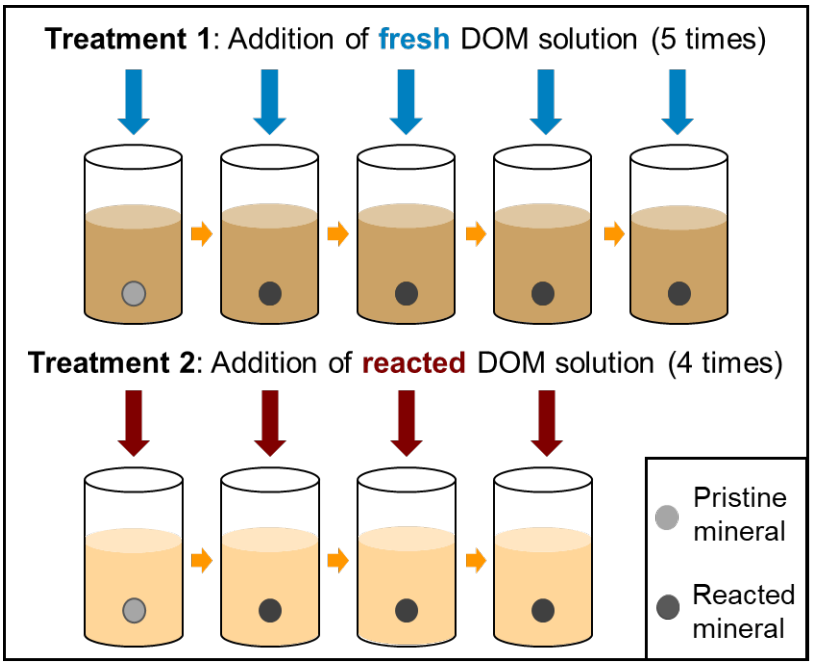

98

99 **Figure 1.** Design of the sequential sorption experiments with repeated addition of fresh and reacted DOM to gibbsite
100 and kaolinite, respectively.

101

102 ## MATERIAL AND METHODS

103 **Minerals and forest floor leachate.** Gibbsite (CAS-number: 21645-51-2) was purchased from
104 Sigma-Aldrich (St. Louis, USA) and kaolinite from Caminauer Kaolinwerke GmbH (Kaolin CF
105 70, Caminau, Germany). They were used as test minerals as they represent prominent groups of
106 secondary soil minerals. The DOM derived from Oa horizon material of a mixed temperate forest
107 dominated by spruce at Tharandt (Dresden, Germany), sampled in March 2019. The material was

sieved to <5 mm, and visible plants and animals were removed. After mixing, the material was frozen at -20°C in sealed polyethylene bags prior to use. Fresh DOM solution for the experiments was prepared by suspending the forest floor material in ultrapure water (1 g in 5 ml H_2O). The suspensions were stirred for 15 minutes, kept for 18 hours at room temperature in the dark, and then filtered through 0.45-µm polyethersulfone membranes (SUPOR-450; Pall Life Science, Dreieich, Germany). The filtrate was diluted with ultrapure water to ~50 mg C l^{-1}. Properties of minerals and DOM solutions are given in Table S1. X-ray diffraction patterns of the used minerals are shown in Figure S1.

Experiment on legacy effects of sorption processes. The main experiment was conducted in a sequential procedure, using either fresh DOM (`$DOM_{fresh}$`; Treatment 1) or reacted DOM (`$DOM_{react}$`; Treatment 2) as outlined in Figure 1. In Treatment 1, an amount of 3.00±0.01 g gibbsite or kaolinite was exposed to five repeated additions of 60 ml of DOM_{fresh} solution. The selection of the mineral-to-solution ratio of 20 (wt./vol.) was based on results of sorption tests using variable mineral-to-solution ratios (Figure S2). We aimed at a DOC sorption of 30-40% of the maximum sorption determined in the pre-experiments after the first DOM_{fresh} addition, so that repeated addition of solutions would allow for gradual accumulation of MOM. After each DOM_{fresh} addition, suspensions were shaken for 1.5 hours to avoid interference from possible microbial processing, then centrifuged (4500 *g* for 30 minutes; ~20°C), and the supernatant solutions carefully decanted. The OM-coated minerals were frosted with liquid nitrogen and freeze-dried. Reacted solutions were then added to appropriate masses of gibbsite or kaolinite (mineral-to-solution ratio kept at 20), and again shaken for 1.5 hours before centrifugation and removal of supernatant. Again, the settled mineral material was frosted with liquid nitrogen and freeze-dried. In total, 15 samples were prepared for the DOM_{fresh} treatment and 12 samples for the DOM_{react}

132 treatment, each in three replicates. Aliquots of the supernatant solutions (15 ml) were immediately
133 analyzed for pH, DOC, and total dissolved nitrogen (N); the remaining solution was frozen in liquid
134 nitrogen and stored at -20°C prior to later analyses.
135
136 **Chemical characterization of initial and reacted organic solutions.** Solutions were
137 analyzed for concentrations of DOC and total dissolved N using a TOC analyzer (TOC-V,
138 Shimadzu Corp., Kyoto, Japan), of Si, Mg, Al, Ca, Na, K, and P by inductively coupled plasma-
139 optical emission spectrometry (Ultima 2, Horiba Jobin-Yvon, Longjumeau, France), and of
140 inorganic N forms (NH_4-N, NO_3-N) and PO_4-P by colorimetric methods using a continuous flow
141 analyzer (ScanPlus, Skalar Analytical B.V., Breda, The Netherlands). Dissolved organic N (DON)
142 was calculated by subtraction of concentrations of inorganic N from those of total dissolved N. The
143 specific UV absorbance at 280 nm ($SUVA_{280}$), a measure for the aromaticity of DOM,[26] was
144 determined using a photometer (SPECORD® 210 PLUS, Analytik Jena AG, Germany).
145 Initial DOM solutions (Table S1) as well as solutions altered by sorption during the first and last
146 addition of the DOM_{fresh} treatment and the first addition of the DOM_{react} treatment were analyzed
147 using ultra-high resolution Fourier-transform ion cyclotron resonance mass spectrometry (FT-ICR-
148 MS; solariX XR, Bruker Daltonics Inc., Billerica, MA, USA), equipped with a dynamically
149 harmonized analyzer cell and a 12T refrigerated actively shielded superconducting magnet (Bruker
150 Biospin, Wissembourg, France). An Apollo II electrospray ionization source was used in negative
151 ion mode (capillary voltage: 4200 V, infusion flow rate: 4 µl min^{-1}). Electrospray ionization in
152 negative mode was chosen due to its high sensitivity for acidic compounds which are major
153 constituents of DOM. Although other ionization methods may provide additional details on distinct
154 DOM fractions, trends observed from ESI(-) measurements of solutions match well with trends
155 observed on particle surfaces measured with laser desorption ionization.[27] For each spectrum, 256

scans were co-added in the mass range 150-1000 m/z with 6-9 ms ion accumulation time and 4 MW time domain (resolution at 400 m/z was ca. 500,000). Mass spectra were internally re-calibrated with a list of peaks (247.0-643.1 m/z, $n > 133$) commonly present in terrestrial DOM and the mass accuracy after linear calibration was better than 0.16 ppm ($n = 24$). Peaks were considered if the signal-to-noise ratio was greater than four. Raw spectra were processed with Compass Data Analysis 5.0 (Bruker Daltonics Inc., Billerica, MA, USA). Molecular formulas (MF) were assigned to peaks in the range 150-750 m/z, allowing for elemental compositions $C_{1-60}H_{0-122}N_{0-4}O_{0-40}S_{0-2}$ with an error range of ± 0.34 ppm (Table S2).[28] The following rules were applied to further constrain MFs: $0.3 \leq H/C \leq 2.5$, $0 \leq O/C \leq 1$, $0 \leq N/C \leq 0.5$, $0 \leq DBE \leq 20$ (double bound equivalent, $DBE = 1 + 1/2\ (2C - H + N)$),[29] $-10 \leq DBE\text{-}O \leq 10$,[30] and element probability rules.[31] Isotopologue formulas (^{13}C, ^{34}S) were used for quality control but removed from the final data set as they represent duplicate chemical information. A process blank for each mineral series was prepared with ultra-pure water and measured in the same way as the samples. Details of the FT-ICR-MS data processing and handling of process blanks are presented in the Supplement (Figure S3-S7, and Table S3-Table S6).

Normalized intensities of the treatment replicates were averaged considering only those molecular formulas present in all three replicates (Table S3, Table S4). The relative sorptivity (RS) of MF was calculated from the averaged and adjusted normalized intensities, according to below given equation for efficiency of MOM formation, and plotted versus H/C and O/C ratios as well as molecular mass. A local polynomial regression was calculated to indicate the relationship between sorptivity and molecular parameters. For each comparison of treatments, only those RS values were considered significant that were outside the 95th percentile (-30% - 20%) of all RS values calculated from the treatment replicates for each mineral series (Figure S5). The RS is, thus, a semi-

quantitative measure of the loss of ion intensity in the solution due to sorption on minerals. Relative sorptivity values > 0% and < 100% indicate a decrease in MF intensity upon sorption, and are considered as sorbed (RS = 100% represents MF that are not detected contact to minerals and are considered fully sorbed), whereas values < 0% and >= -100% indicate an increase in MF intensity after contact to minerals, and are regarded as desorbed or released from the surface. Formulas with RS values < -100% or not present in the initial DOM solution were set to -100%.

Characterization of pristine and coated mineral surfaces. Surface accumulation of C as well as C species at the mineral surfaces were assessed using X-ray photoelectron spectroscopy (XPS; Axis Supra, Kratos Analytical, Manchester, UK). Freeze-dried mineral powders (initial minerals, and minerals sampled after the first and last addition of DOM of both treatments) were mounted on indium foil (99.99%, Plano GmbH, Wetzlar, Germany). The subsequent XPS analyses included (i) wide scans (0-1200 eV), from which the C 1s signal of C (at 284.8 eV) was used to correct the binding energies, and (ii) detail scans of the C 1s region (277-304 eV) in order to deduce the abundance of C species.[32] With the collimator set to slot mode, three randomly selected positions of 300 × 700 µm (width × length) were radiated and analyzed per sample. Instrument conditions were: emission current of 15 mA (wide scans) or 25 mA (detail scans), step size of 1 eV (wide scans) or 0.1 eV (detail scans), pass energy of 160 eV (wide scans) or 20 eV (detail scans), and up to five sweeps. Surface concentrations for all detected elements are given in the Supplement (Table S7). The C 1s peak was deconvoluted for analysis of C species of variable oxidation states. We considered peaks at 284.8 eV (±0.1) indicative for C-C and C-H type C (denoted here as C1), 286.4 eV (±0.1) for C-O and C-N (C2), 287.9 eV (±0.1) for C=O and O-C-O (C3), and 289.3 eV (±0.1) for O=C-O and O=C-N (C4), respectively.[32] The full-width-at-half-maximum of the peaks was allowed to vary between 1.0 and 1.5. The fitting procedure used a linear

background approximation and a Gaussian-Lorentzian ratio of 0.3. Electrophoretic mobility for fresh and OM-coated minerals in aqueous suspension (21°C) were measured in triplicates using a zeta (ζ) potential analyzer (Nano-ZS, Malvern Panalytical, Malvern, UK), and ζ potentials were derived on basis of the Smoluchowski model. Prior to measurements, pH values of suspensions were adjusted to 4.5 and 6.5, respectively, in order to assess the ζ potential at the range of pH values measured in the main experiment.

Calculations and statistics. The efficiency of MOM formation was calculated by Equation 1, indicating the net MOM formation per amount of DOC input (i.e., the MOM formation efficiency is the nest result of both, sorption and desorption of organic molecules),[6] where DOC_i is the DOC concentration of input solutions and DOC_f the final concentration after sorption (mg C l^{-1}):

$$\textit{Efficiency of MOM formation}\ (\%) = (DOC_i - DOC_f) / DOC_i \times 100\% \quad \text{(Eq. 1)}$$

Statistical tests, including ANOVA and pairwise comparison procedures (Holm-Sidak tests and t-tests), were conducted using SigmaPlot version 10.0 (Systat Software GmbH). The analyses also included tests on assumptions of the parametric tests (normality and constant variance).

RESULTS

Efficiency of formation of mineral-associated organic matter. The efficiency of MOM formation decreased with number of solution additions for all experimental settings, i.e., two types of minerals and treatments (Figure 2). Yet, pattern and extent of the decrease differed between settings. When DOM_{fresh} was added to gibbsite, the efficiencies decreased significantly ($p<0.001$; Holm-Sidak test) from 25.2±0.4% for the first (which corresponds to a decrease in DOC concentration from 42 to 31 mg l^{-1}; not shown) to 3.6±1.4% for the second solution addition, and

it was close to zero for additions 3 to 5 (i.e., 0.5±0.7% on average for the 3 additions). After five DOM_{fresh} additions, the cumulative amount of C sorbed to gibbsite averaged 254±27 µg C g^{-1}, or 195±21 µg C m^{-2}, of which on average 83% was already reached after the first addition (Figure 2). In comparison, after five DOM_{fresh} additions to kaolinite, the cumulatively sorbed C was 400±36 µg C g^{-1}, or 27±3 µg C m^{-2}, with 59% of this value being reached after the first addition (Figure 2). An approximately seven times higher C accumulation per surface area demonstrated that gibbsite was much more effective in MOM formation than kaolinite.

For gibbsite, we found similar efficiencies in MOM formation for the first DOM_{react} (Treatment 2) as for the first DOM_{fresh} addition (Treatment 1) (Figure 2; p=0.873, t-test), showing that sorption-induced changes in solution properties in Treatment 1 (including changes in DOM composition, Figure 3, and a pH increase from 4.6 to 6.3, Figure 4,) had little effect on the subsequent C sorption. The decrease in MOM formation efficiencies upon repeated DOM_{react} addition, however, was less pronounced than for the repeated addition of DOM_{fresh}.

For kaolinite, we found (in contrast to gibbsite) that the MOM formation efficiency for the first DOM_{react} addition was significantly lower than for the first DOM_{fresh} addition (on average by 53% larger; p=0.013). At repeated DOM_{react} addition, the efficiencies decreased on average (from 11% at the first to 4% at the fourth addition), but no significant differences between the four DOM_{react} additions were found (p=0.8; repeated measures ANOVA).

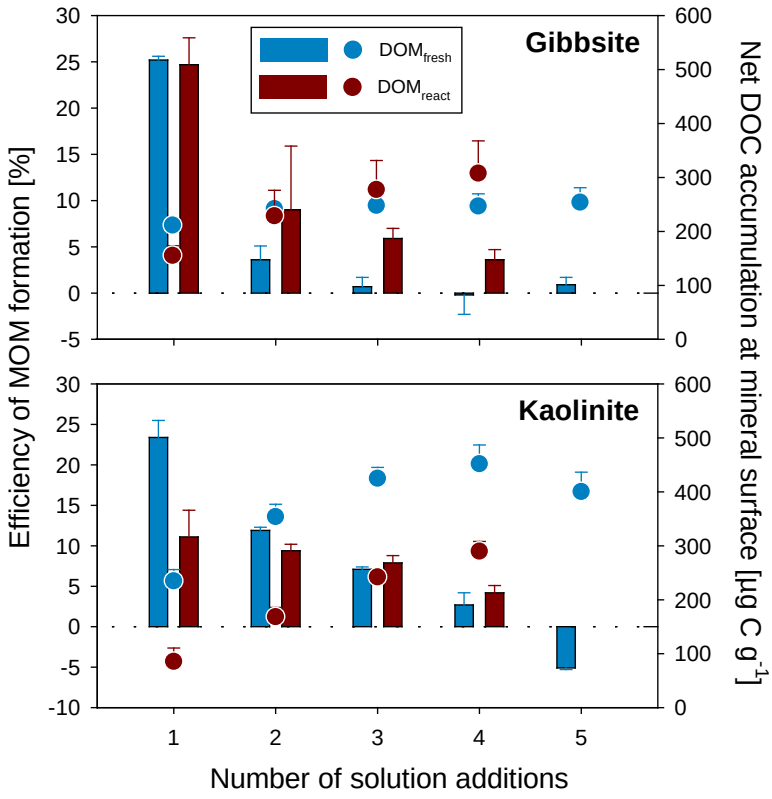

Figure 2. Efficiencies of MOM formation (bars) and net DOC accumulation at mineral surfaces (dots) across repeated additions of fresh DOM solution (DOM_{fresh}; Treatment 1, 5 additions in total) or reacted DOM solution (DOM_{react}; Treatment 2, 4 additions in total). Error bars represent standard deviations of the mean (n = 3).

Changes in solution composition during sorption events. The FT-ICR-MS data provide a molecular-level view of sorption-induced alterations of the DOM composition. The initial DOM solution was characterized by a large fraction of CHO (84%) and CHNO (14%) compounds. Sulfur-containing compounds contributed only minor to the peak number and intensity (<1%, Table S3) and are not considered further. Overall, the number of MF and spectral intensity decreased with decreasing concentrations of DOC after sorption (Table S3). Considering the relative decrease in peak intensities, expressed as RS, 14-78% of CHO and 17-75% of CHNO MF showed significant (0% < RS < 100%) or complete sorption (RS = 100%), with large differences between experiments (Table S5, Table S6). Strongest sorption across MF was found for the first

256 additions of DOM_{fresh} (72-77%) and DOM_{react} (26-61%), while only few MF (<15%) showed

257 significant sorption in both mineral series upon the fifth addition of DOM_{fresh} (Figure S8, Figure

258 S9). Generally, the sorbed fraction of CHO MF was larger than of CHNO MF, but for CHNO MF

259 complete sorption was more common (Table S6). In all experiments, a fraction of MF (3-15%) in

260 solution was either strongly enriched (RS > -100%) or only detected after sorption (Table S6).

261 Those MF may represent compounds additionally released or desorbed from the minerals and were

262 not detected in the initial solution.

263

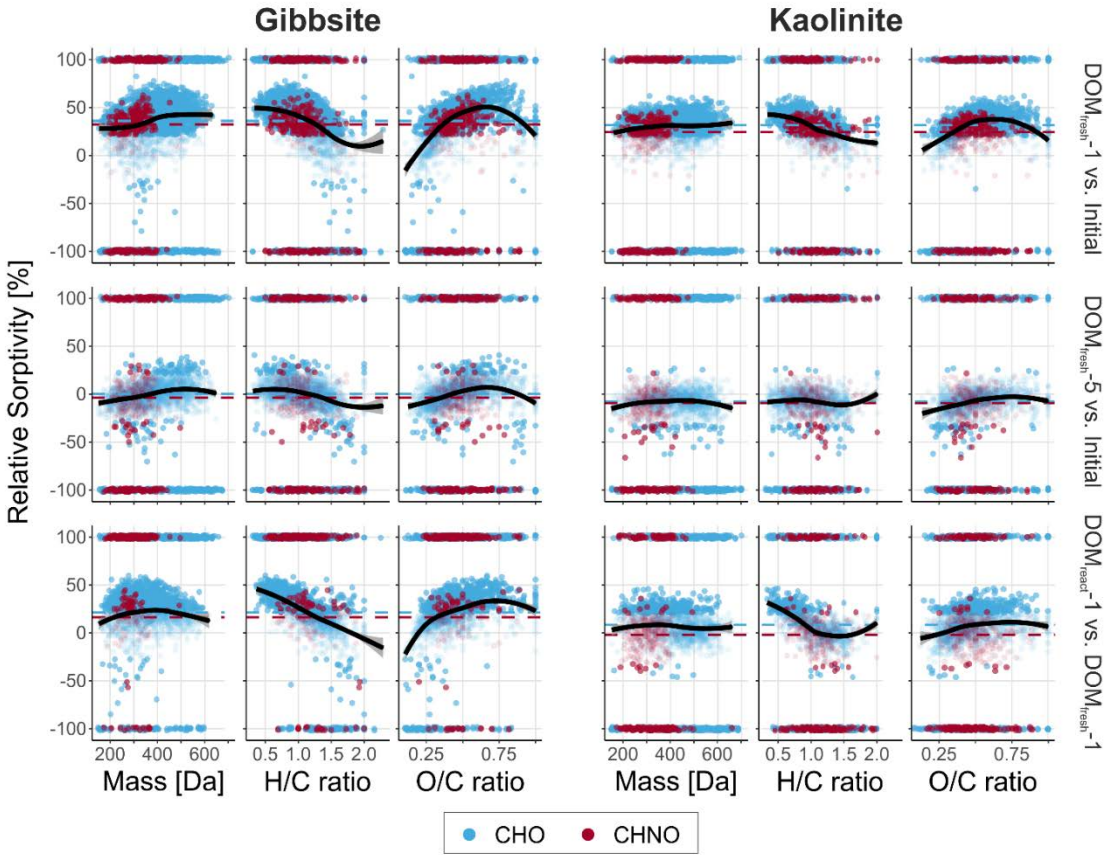

273 **Figure 3**: Relative sorptivity (RS) of molecules in sorption experiments as assessed with FT-ICR-MS. The RS values
274 are plotted versus molecular mass and molecular H/C and O/C ratios. Significantly sorbing (RS > 0%) or desorbing
275 (RS < 0%) molecules are indicated as fully opaque dots and a local polynomial regression fit with 95% confidence
276 interval is shown as black curve. Molecules sorbing completely (RS = 100%) or not present in the initial samples (RS
277 = -100%) are also displayed. CHO (blue) and CHNO (red) compound classes are shown and the mean RS value for
278 CHO and CHNO molecules are indicated as dashed lines.

Sorption-induced alterations of DOM were also indicated by ratios of DOC to DON and $SUVA_{280}$ values (Figure 4). Most sorption events caused reductions of both values; changes in DOC to DON ratios ranged from -3 to -37% for gibbsite, and from -4 to -20% for kaolinite. Likewise, we found changes of average $SUVA_{280}$ values ranging from 0 to -29% for gibbsite, and from -4 to -46% for kaolinite. These data suggest that N-poor aromatic components preferentially sorbed to mineral surfaces throughout the experiment and irrespective of legacy effects form previous sorption events.

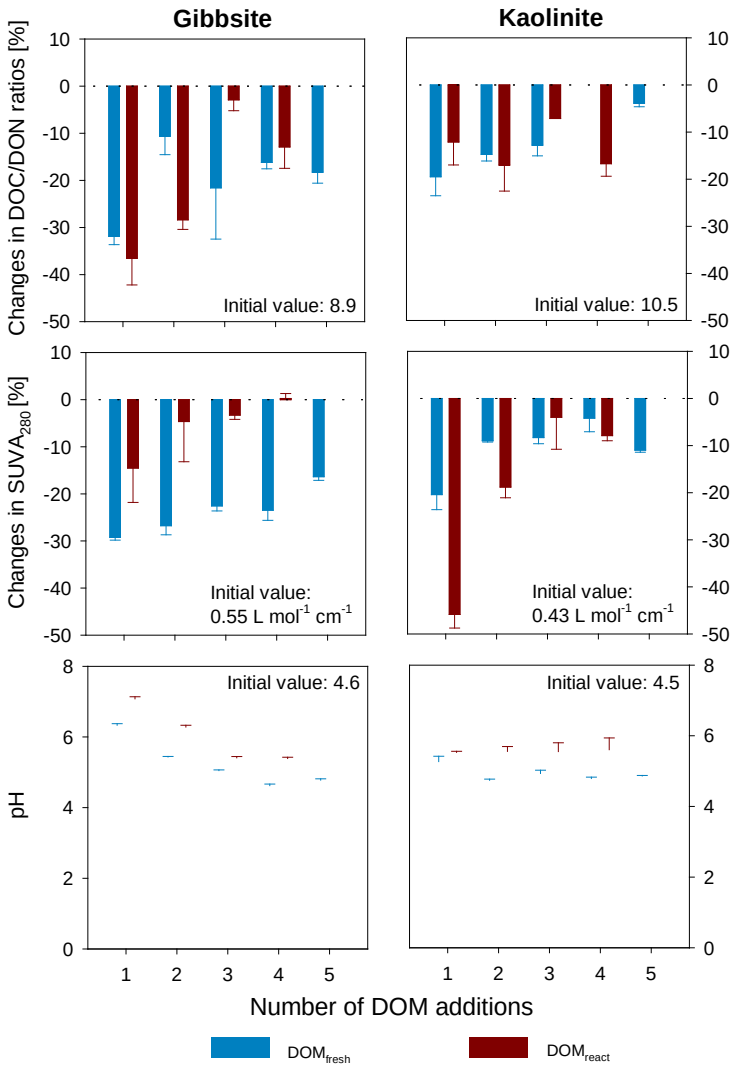

Figure 4. Sorption-induced alterations of DOM solutions (i.e., relative changes in DOC/DON and $SUVA_{280}$; changes in pH) across repeated solution additions (DOM_{fresh}; Treatment 1, 5 additions in total) or reacted DOM (DOM_{react}; Treatment 2, 4 additions in total). Error bars represent standard deviations of the mean (n = 3).

Mineral surface changes due to sorption events. We gained insight into the chemistry of sorbed organic compounds via direct assessment of surfaces using XPS. For pristine minerals, average C concentrations of 4.9 atom-% (gibbsite) and 5.5 atom-% (kaolinite) were determined (Table S1), indicating the presence of adventitious C. Such ubiquitous contamination typically includes low-oxidized organic molecules from the atmosphere.[33] For gibbsite, we noted significant (paired t-tests; $p<0.05$) increases in average C concentrations at the mineral surfaces upon the first addition of DOM_{fresh} (13.2 atom-%) or DOM_{react} (12.0 atom-%). Surface C concentrations did not change anymore after the first additions (Figure 4). The detection of Al after five DOM_{fresh} and four DOM_{react} additions (~15 atom-%; Table S7) suggests that at the end of the experiments, the gibbsite surfaces were either not completely covered with OM and/or the coating was less than about 10 nm thick.[34] No N peaks were detected (not shown), which was in line with solution data, indicating low sorptivity of N-containing organic molecules (Figure 3). The relative contribution of surface C-C and C-H type C to the total C 1s peak (Figure 4) decreased upon solution addition in both treatments (however, according to results of paired t-tests the decreases were not statistically significant except for the decrease from the first to fourth DOM_{react} addition), and the contribution of O=C-O type C remained nearly constant across the sorption experiments. In turn, significant increases in relative contributions of C-O type C for the first addition of DOM in both treatments and the first and fourth addition in Treatment 2 were observed. In addition, the increase of C=O and O-C-O type C was significant for the first addition of DOM in both treatments.

For kaolinite, the surface C concentrations increased only slightly after the first DOM addition in Treatment 1 and 2, while only for Treatment 2 a clear increase upon the first DOM_{react} addition was noted (from 5.5 to 7.6 atom-%, paired t-tests, $p=0.048$). No clear trends in C form distributions with repeated addition of DOM solutions were found for kaolinite (Figure 5). Overall, the C

concentrations at the mineral surfaces as revealed by XPS were well in line with the differences in sorptivity between the two mineral surfaces as indicated by the amounts of DOC removed from solutions per unit surface area. For gibbsite, we also found clear decreases in ζ potentials (measured at pH 4.5 or 6.5) upon addition of DOM (Figure 6). Initially positive ζ potentials became negative already after the first DOM addition, while only for analyses at pH 4.5 the decrease in ζ potentials depended on treatment (i.e., it was greater for DOM_{fresh} than for DOM_{react} additions). In contrast, the initially negative ζ potentials of kaolinite were not affected by the DOM additions (Figure 6).

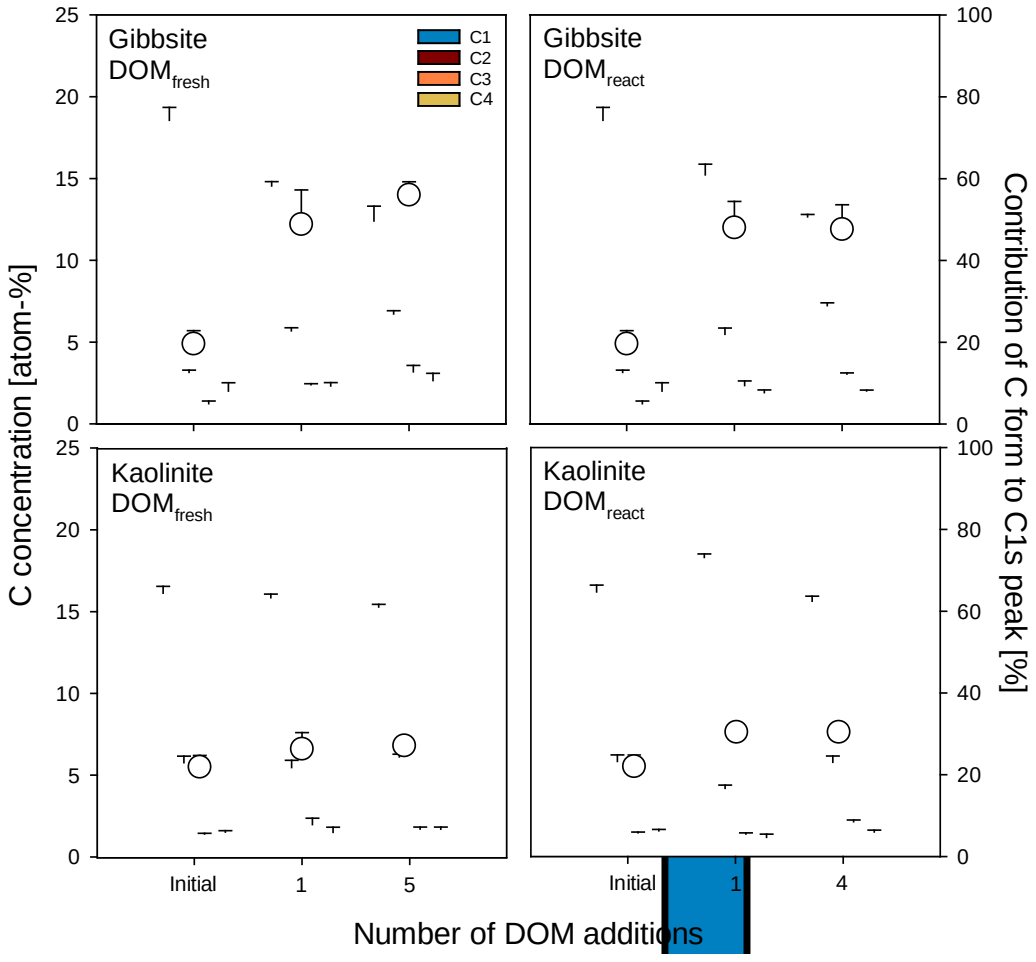

Figure 5. XPS data showing C concentrations (dots) of different C forms as well as contribution of different C forms (C-C and C-H type C, denoted as C1; C-O and C-N type C, denoted as C2; C=O and O-C-O type C, denoted as C3; O=C-O and O=C-N type C, denoted as C4) to the C1s peak (bars) across repeated solution additions (DOM_{fresh};

Treatment 1, 5 additions in total) or reacted DOM (DOM_{react}; Treatment 2, 4 additions in total). Error bars represent standard deviations of the mean (n = 3).

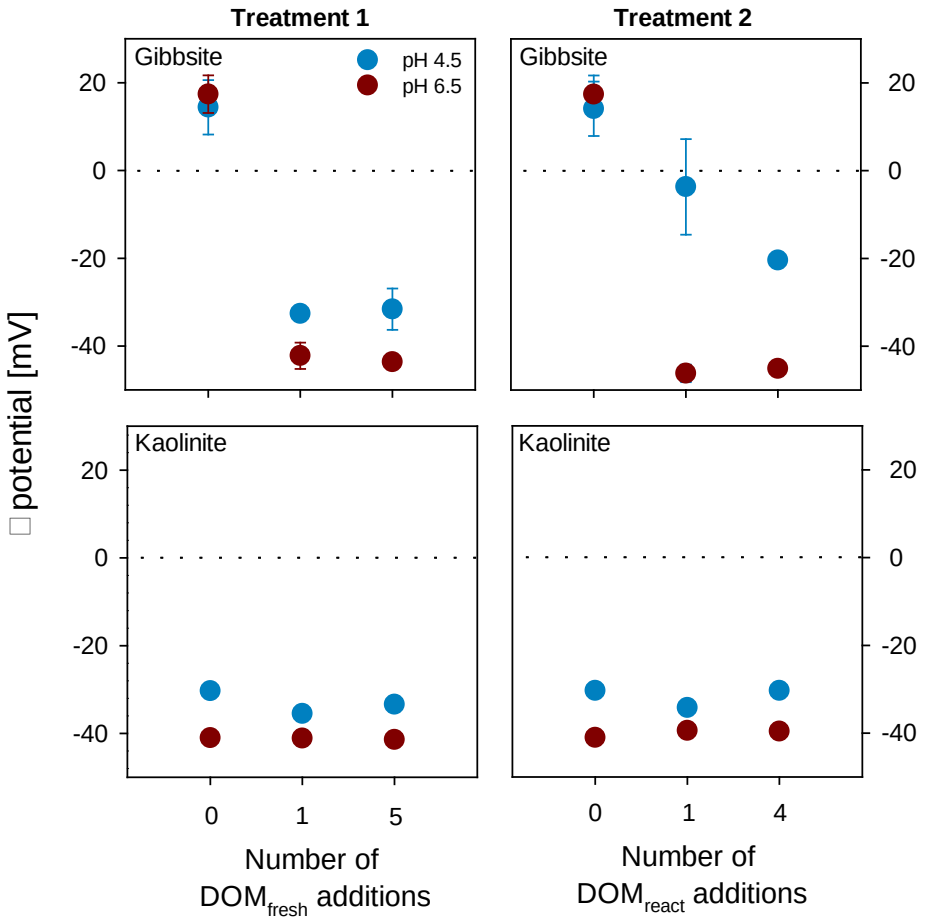

Figure 6 ζ potentials (analyzed at pH 4.5 or 6.5) across repeated solution additions (DOM_{fresh}; Treatment 1, 5 additions in total) or reacted DOM (DOM_{react}; Treatment 2, 4 additions in total). Error bars represent standard deviations of the mean (n = 3).

DISCUSSION

While sorption patterns differed between minerals and treatments, the general observation of decreasing efficiencies of MOM formation during repeated DOM_{fresh} or DOM_{react} addition (Figure 2) demonstrate the importance of the availability of pristine mineral surfaces for MOM formation in soil. The pristine gibbsite surfaces were initially much more reactive than those of kaolinite, but for both minerals the MOM formation efficiencies dropped close to zero at later DOM additions. This implies that it is not necessarily content, surface area, and type of sorptive minerals that

338 determines present efficiencies of MOM formation at a site, but rather the rate at which pristine
339 surfaces form and come in contact with DOM. This view is supported by findings of field studies
340 showing that C levels and abundance of reactive secondary minerals increase most quickly during
341 early soil development and hardly change in old soil.[2,35-37]

342 Decreasing efficiencies of MOM formation can be explained by the interplay between different
343 factors. First, organic molecules sorbed to mineral surfaces occupy binding sites and render them
344 unavailable at repeated DOM addition. Second, formation of OM coatings at gibbsite surfaces
345 reversed the surface charge already upon the first DOM_{fresh} or DOM_{react} addition (Figure 5), a result
346 also reported in studies using various other metal oxide and natural OM samples.[38-41] Consequently,
347 negatively charged DOM components with high affinity for pristine mineral surfaces are prevented
348 approaching sorption sites upon repeated DOM additions due to electrostatic repulsion.[42] This may
349 explain why even after repeated DOM addition, with no more net C accumulation at surfaces,
350 Strong contributions of Si and/or Al to XPS spectra/Table S7) suggested that mineral surfaces were
351 not fully covered with OM. The repulsion mechanism may also have affected MOM formation in
352 experiments with kaolinite despite no detectable changes in ζ potentials. Probably, organic
353 molecules were mainly bound to aluminol sites of kaolinite, while its siloxane surfaces, usually
354 characterized by negative ζ potential were less sorptive.[43,44] This would explain (i) the overall
355 lower DOM sorption of the kaolinite surface and (ii) that in general the trends of sorption-induced
356 DOM fractionation were comparable for the two minerals (Figures 3 and 4). The ζ potential as well
357 as XPS analyses assessed the bulk surface of the samples, but seem not sensitive enough to capture
358 the MOM formation at the kaolinite edges, which represent only a fraction of the total surface.

359 Pronounced sorption-induced DOM fractionation found for the first DOM_{fresh} and DOM_{react}
360 additions (Figures 3 and 4) basically suggests that DOM components differed in their strength to

bind directly to the mineral surface.[45,46] At the first DOM addition, DOM compounds with relatively low H/C ratio, high O/C ratio (Figure 3), and/or low N content (Figure 4, decreasing DOC/DON) were preferentially sorbed. These compounds are primarily derived from plants rather than microbes, e.g., aromatics, low-N and/or carboxyl-rich components.[12,47] In natural soil, direct microbial growth on mineral surfaces could lead to larger contributions of microbial metabolites to MOM than in situation where interface interactions are controlled by sorption, as in our study.[6] It has oftentimes been reported that aromatic DOM compounds (e.g., tannins and depolymerization products of lignin) are prone to bind to secondary minerals in soil.[12,13,23,48,49] The $SUVA_{280}$ data also suggest decreasing aromaticity of DOM upon sorption (Figure 4). The decreasing DOC/DON values upon sorption as well as the high relative sorptivity of molecules with a low H/C and high O/C ratio (Figure 3) may also partly be explained by selective sorption of plant-derived aromatics. High abundance of hydroxyl and/or carboxyl groups presumably caused the high sorptivity of the aromatic compounds. Presence of these groups at the mineral surfaces was indicated by solution-based FT-ICR-MS analyses (high sorptivity of O-containing molecules; Figure 3) and, for gibbsite, XPS analysis (increasing amounts of O=C-O type C as well as C=O and O-C-O type C at the surfaces upon DOM addition; Figure 5). Hydroxyl- and/or carboxyl-rich compounds sorb to positively charged aluminol sites via outersphere or innersphere complexes.[4] As innersphere complex formation proceeds via ligand exchange releasing H_2O or OH^- from mineral surfaces into solution,[4,50] it explains the increasing pH particularly at the first DOM_{fresh} and DOM_{react} additions (Figure 3). The formation of innersphere complexes will likely hamper desorption of the preferentially sorbed DOM compounds, and thus, support their stabilization against microbial decay.[45] Occupation of binding sites by sorbing organic molecules explains the decreasing MOM formation efficiencies at repeated DOM addition. The reversal of the gibbsite's surface charge

384 indicates that not all negatively charged functional groups of the sorbing organic molecules become
385 involved in surface bonds.

386 Even at later DOM additions, when little or no more net C accumulation at surfaces was found, we
387 still noted pronounced DOM alterations during sorption events (Figure 3 and 4), which can only
388 be explained by exchange reactions between sorbed and dissolved organic molecules.[13,51] The exact
389 chemical mechanism of such exchange reactions is still not fully resolved. Our data suggest that
390 molecules preferentially sorbing at repeated DOM additions had similar features as those sorbing
391 at the first DOM additions. Indications for this are the decreased $SUVA_{280}$ and the DOC/DON
392 ratios at repeated DOM additions (Figure 4) and the similar distribution of RS values across the
393 molecular properties for the first as well as for the fifth DOM addition (Figure 3). We therefore
394 presume that the surface exchange is due to different sorption affinities of organic molecules, i.e.,
395 the most sorptive compounds replaced less sorptive ones. Notably, while the exchange processes
396 had significant effects on DOM composition, they seemingly did not change MOM formation
397 efficiencies at later DOM additions.

398 One focus of our study was the role of organic-organic interactions (i.e., sorption of DOM
399 components onto OM coatings) for MOM accumulation. The FT-ICR-MS data showed that also
400 some potentially more hydrophobic components with low O contents sorbed preferentially (Figure
401 3), and also aromatic moieties can theoretically sorb via hydrophobic interactions (e.g., dipole-
402 dipole, dipole-induced-dipole, dispersive forces, and Π-Π interactions) to pre-sorbed OM, [52] which
403 would contribute to the decreasing $SUVA_{280}$ values (Figure 4). In addition, polyvalent inorganic
404 cations were present in the DOM solutions (Table S1), and thus, ion bridges between organic
405 molecules and mineral surfaces might have formed as well.[4,53] Nevertheless, our data suggest that
406 organic-organic interactions played a minor role as regulators of efficiencies of MOM formation

at continuous DOM input. The view is supported by various observations. Foremost, inter-organic interactions should cause MOM coatings to grow even at later DOM additions as sorption sites are continuously established at pre-formed MOM, but this was not observed. Also, we did not find evidence of pronounced changes in (i) patterns of DOM fractionation (Figures 3 and 4), (ii) composition of MOM (XPS analyses, Figure 5), and (iii) surface charge (ζ potentials, Figure 6) when DOM was repeatedly added to OM-coated minerals. The legacy effect of sorption-induced alterations of solution in subsequent sorption events was controlled by mineral surface properties. Addition of both DOM_{react} and DOM_{fresh} resulted in similar efficiencies of MOM formation at pristine gibbsite surfaces, while the efficiencies at the kaolinite surfaces were reduced for the DOM_{react} addition (Figure 2). This finding may be explained by the higher sorptivity of gibbsite surfaces, at which also addition of DOM already depleted in the most strongly sorbing compounds induced efficient formation of MOM. This implies that in subsoils the efficiency of MOM formation from DOM already altered by sorption during passage of overlying horizons is more restricted to the most sorptive minerals than in the topsoils.

Environmental implication. Our work provides explanations for observed differences in efficiencies of MOM formation across ecosystems. The efficiencies appear to be strongly determined by very first sorptive interactions of DOM solutions with pristine mineral surfaces. These initial sorption events drastically reduce the sorptivity of the resulting mineral-organic surfaces, so that the efficiencies drop to zero within few sorption events. Consequently, high MOM formation rates are strongly favored in soils where large amounts of pristine sorptive mineral surfaces meet DOM, e.g., in soils developing from highly weatherable rock substrate, supporting rapid formation of sorptive secondary minerals.[3] In terms of soil C management, profound changes in vegetation and/or OM input rates can promote MOM formation if they enhance the formation

rates of sorptive secondary mineral.[54] Management may also affect soil structure turnover by stimulating macro-faunal burrowing activity,[55] and thus, likewise enhance the accessibility of mineral surfaces to OM. Increasing the plant litter input might also support MOM formation by increased transfer of DOM into subsoil horizon,[56] which usually offer more pristine, or less OM-coated mineral surfaces than topsoils. Recent work, however, suggests that this might require tremendous input of litter material.[57] Therefore, the probably best opportunities for increasing MOM are to promote organic C input to (i) topsoils that have partly lost their OM coatings due to long-term arable use, (ii) soils that expose subsoil mineral surfaces due to erosion of OM-rich topsoils, and (iii) soils that have their contents of pristine sorptive minerals increased by human activities, such as after soil drainage. This is well in line with ideas of previous research,[58] pointing out that young and especially eroded soils offer the highest potential for an efficient built-up of MOM, which concurrently improves soil quality and contributes to efforts of mitigating the atmosphere's rising CO_2 level.

AUTHOR INFORMATION

Corresponding author

Shuling Chen, slchen@cug.edu.cn, Phone: +8618064077782

Notes

The authors declare no competing financial interest.

ACKNOWLEDGEMENTS

This work was funded by the German Research Foundation (DFG, project "Formation and properties of mineral-organic soil interfaces as revealed by X-ray photoelectron spectroscopy", MI

1377/13-1). Additional support was from the Program for Guangdong Introducing Innovative and Entrepreneurial Teams (2017ZT07Z479) and Natural Science Foundation of China (No.41772032, No.42172045). We are grateful for the help of Anika Klotzbücher, Alexandra Boritzki, Christine Krenkewitz, and Gudrun von Koch during laboratory work. We thank Jan Kaesler for the FT-ICR-MS measurements and Kai Franze for software development. The authors are grateful for using the analytical facilities of the Centre for Chemical Microscopy (ProVIS) at the Helmholtz Centre for Environmental Research, Leipzig which is supported by the European Regional Development Funds (EFRE - Europe funds Saxony) and the Helmholtz Association.

Supporting Information Available

This information is available free of charge via the Internet at http://pubs.acs.org.

Data processing of FT-ICR-MS, properties of minerals and DOM solution used in this study, preliminary experiments, surface element distribution by XPS.

REFERENCES

(1) Minasny, B.; Malone, B. P.; McBratney, A. B.; Angers, D. A.; Arrouays, D.; Chambers, A.; Chaplot, V.; Chen, Z.-S.; Cheng, K.; Das, B. S.; Field, D. J.; Gimona, A.; Hedley, C. B.; Hong, S. Y.; Mandal, B.; Marchant, B. P.; Martin, M.; McConkey, B. G.; Mulder, V. L.; O'Rourke, S.; Richer-de-Forges, A. C.; Odeh, I.; Padarian, J.; Paustian, K.; Pan, G.; Poggio, L.; Savin, I.; Stolbovoy, V.; Stockmann, U.; Sulaeman, Y.; Tsui, C.-C.; Vågen, T.-G.; van Wesemael, B.; Winowiecki, L., Soil carbon 4 per mille. *Geoderma* **2017,** *292*, 59-86.

(2) Mikutta, R.; Turner, S.; Schippers, A.; Gentsch, N.; Meyer-Stüve, S.; Condron, L. M.; Peltzer, D. A.; Richardson, S. J.; Eger, A.; Hempel, G.; Kaiser, K.; Klotzbücher, T.; Guggenberger, G., Microbial and abiotic controls on mineral-associated organic matter in soil profiles along an ecosystem gradient. *Sci. Rep.* **2019,** *9* (1), 10294.

(3) Torn, M. S.; Trumbore, S. E.; Chadwick, O. A.; Vitousek, P. M.; Hendricks, D. M., Mineral control of soil organic carbon storage and turnover. *Nature* **1997,** *389* (6647), 170-173.

(4) Kleber, M.; Eusterhues, K.; Keiluweit, M.; Mikutta, C.; Mikutta, R.; Nico, P. S., Chapter one - mineral–organic associations: Formation, properties, and relevance in soil environments. In *Adv. Agron.*, Sparks, D. L., Ed. Academic Press: **2015**; Vol. 130, pp 1-140.

(5) Kögel-Knabner, I.; Guggenberger, G.; Kleber, M.; Kandeler, E.; Kalbitz, K.; Scheu, S.; Eusterhues, K.; Leinweber, P., Organo-mineral associations in temperate soils: Integrating biology, mineralogy, and organic matter chemistry. *J. Plant Nutr. Soil Sci.* **2008,** *171* (1), 61-82.

(6) Cotrufo, M. F.; Wallenstein, M. D.; Boot, C. M.; Denef, K.; Paul, E., The microbial efficiency-matrix stabilization (mems) framework integrates plant litter decomposition with soil organic matter stabilization: Do labile plant inputs form stable soil organic matter? *Global Change Biol.* **2013,** *19* (4), 988-995.
(7) Castellano, M. J.; Mueller, K. E.; Olk, D. C.; Sawyer, J. E.; Six, J., Integrating plant litter quality, soil organic matter stabilization, and the carbon saturation concept. *Global Change Biol.* **2015,** *21* (9), 3200-3209.
(8) Lavallee, J. M.; Soong, J. L.; Cotrufo, M. F., Conceptualizing soil organic matter into particulate and mineral-associated forms to address global change in the 21st century. *Global Change Biol.* **2020,** *26* (1), 261-273.
(9) Cotrufo, M. F.; Soong, J. L.; Horton, A. J.; Campbell, E. E.; Haddix, Michelle L.; Wall, D. H.; Parton, W. J., Formation of soil organic matter via biochemical and physical pathways of litter mass loss. *Nat. Geosci.* **2015,** *8* (10), 776-779.
(10) Kaiser, K.; Kalbitz, K., Cycling downwards-dissolved organic matter in soils. *Soil Biol. Biochem.* **2012,** *52*, 29-32.
(11) Kalbitz, K., Controls on the dynamics of dissolved organic matter in soils: A review. *Soil Sci.* **2000,** *165* (4), 277-304.
(12) Kramer, M. G.; Sanderman, J.; Chadwick, O. A.; Chorover, J.; Vitousek, P. M., Long-term carbon storage through retention of dissolved aromatic acids by reactive particles in soil. *Global Change Biol.* **2012,** *18* (8), 2594-2605.
(13) Sanderman, J.; Amundson, R., A comparative study of dissolved organic carbon transport and stabilization in california forest and grassland soils. *Biogeochemistry* **2008,** *89* (3), 309-327.
(14) Six, J.; Conant, R. T.; Paul, E. A.; Paustian, K., Stabilization mechanisms of soil organic matter: Implications for c-saturation of soils. *Plant Soil* **2002,** *241* (2), 155-176.
(15) Stewart, C. E.; Paustian, K.; Conant, R. T.; Plante, A. F.; Six, J., Soil carbon saturation: Concept, evidence and evaluation. *Biogeochemistry* **2007,** *86* (1), 19-31.
(16) Abramoff, R. Z.; Georgiou, K.; Guenet, B.; Torn, M. S.; Huang, Y.; Zhang, H.; Feng, W.; Jagadamma, S.; Kaiser, K.; Kothawala, D.; Mayes, M. A.; Ciais, P., How much carbon can be added to soil by sorption? *Biogeochemistry* **2021,** *152* (2-3), 127-142.
(17) Coward, E. K.; Ohno, T.; Plante, A. F., Adsorption and molecular fractionation of dissolved organic matter on iron-bearing mineral matrices of varying crystallinity. *Environ Sci Technol* **2018,** *52* (3), 1036-1044.
(18) Mitchell, P. J.; Simpson, A. J.; Soong, R.; Simpson, M. J., Nuclear magnetic resonance analysis of changes in dissolved organic matter composition with successive layering on clay mineral surfaces. *Soil Systems* **2018,** *2* (1), 8.
(19) Possinger, A. R.; Zachman, M. J.; Enders, A.; Levin, B. D. A.; Muller, D. A.; Kourkoutis, L. F.; Lehmann, J., Organo-organic and organo-mineral interfaces in soil at the nanometer scale. *Nature Communications* **2020,** *11* (1), 6103.
(20) Vogel, C.; Mueller, C. W.; Höschen, C.; Buegger, F.; Heister, K.; Schulz, S.; Schloter, M.; Kögel-Knabner, I., Submicron structures provide preferential spots for carbon and nitrogen sequestration in soils. *Nature Communications* **2014,** *5* (1), 2947.
(21) Gao, J.; Mikutta, R.; Jansen, B.; Guggenberger, G.; Vogel, C.; Kalbitz, K., The multilayer model of soil mineral–organic interfaces-a review. *J. Plant Nutr. Soil Sci.* **2020,** *183* (1), 27-41.
(22) Kleber, M.; Sollins, P.; Sutton, R., A conceptual model of organo-mineral interactions in soils: Self-assembly of organic molecular fragments into zonal structures on mineral surfaces. *Biogeochemistry* **2007,** *85* (1), 9-24.
(23) Klotzbücher, T.; Kalbitz, K.; Cerli, C.; Hernes, P. J.; Kaiser, K., Gone or just out of sight? The apparent disappearance of aromatic litter components in soils. *SOIL* **2016,** *2* (3), 325-335.
(24) Roth, V.-N.; Lange, M.; Simon, C.; Hertkorn, N.; Bucher, S.; Goodall, T.; Griffiths, R. I.; Mellado-Vázquez, P. G.; Mommer, L.; Oram, N. J.; Weigelt, A.; Dittmar, T.; Gleixner, G., Persistence of dissolved organic matter explained by molecular changes during its passage through soil. *Nat. Geosci.* **2019,** *12* (9), 755-761.

(25) Lehmann, J.; Kleber, M., The contentious nature of soil organic matter. *Nature* **2015,** *528* (7580), 60-68.
(26) Chin, Y. P.; Aiken, G.; O'Loughlin, E., Molecular weight, polydispersity, and spectroscopic properties of aquatic humic substances. *Environ. Sci. Technol.* **1994,** *28* (11), 1853-1858.
(27) Giannopoulos, K.; Benettoni, P.; Holbrook, T.; Reemtsma, T.; Wagner, S.; Lechtenfeld, O. J., Direct analysis of fulvic acids adsorbed onto capped gold nanoparticles by laser desorption ionization fourier-transform ion cyclotron resonance mass spectrometry. Environ. Sci. Nano. **2021**, *8*, 2336-2346.
(28) Lechtenfeld, O. J.; Kattner, G.; Flerus, R.; McCallister, S. L.; Schmitt-Kopplin, P.; Koch, B. P., Molecular transformation and degradation of refractory dissolved organic matter in the atlantic and southern ocean. *Geochim. Cosmochim. Acta* **2014,** *126*, 321-337.
(29) Koch, B. P.; Kattner, G.; Witt, M.; Passow, U., Molecular insights into the microbial formation of marine dissolved organic matter: Recalcitrant or labile? *Biogeosciences* **2014,** *11* (15), 4173-4190.
(30) Herzsprung, P.; Hertkorn, N.; von Tümpling, W.; Harir, M.; Friese, K.; Schmitt-Kopplin, P., Understanding molecular formula assignment of fourier transform ion cyclotron resonance mass spectrometry data of natural organic matter from a chemical point of view. *Anal. Bioanal. Chem.* **2014,** *406* (30), 7977-7987.
(31) Kind, T.; Fiehn, O., Seven golden rules for heuristic filtering of molecular formulas obtained by accurate mass spectrometry. *BMC Bioinform.* **2007,** *8* (1), 105.
(32) Gerin, P. A.; Genet, M. J.; Herbillon, A. J.; Delvaux, B., Surface analysis of soil material by x-ray photoelectron spectroscopy. *Eur. J. Soil Sci.* **2003,** *54* (3), 589-604.
(33) Barr, T. L.; Seal, S., Nature of the use of adventitious carbon as a binding energy standard. *J. Vac. Sci. Technol. A* **1995,** *13* (3), 1239-1246.
(34) Woche, S. K.; Goebel, M.-O.; Mikutta, R.; Schurig, C.; Kaestner, M.; Guggenberger, G.; Bachmann, J., Soil wettability can be explained by the chemical composition of particle interfaces - an xps study. *Sci. Rep.* **2017,** *7* (1), 42877.
(35) Doetterl, S.; Berhe, A. A.; Arnold, C.; Bodé, S.; Fiener, P.; Finke, P.; Fuchslueger, L.; Griepentrog, M.; Harden, J. W.; Nadeu, E.; Schnecker, J.; Six, J.; Trumbore, S.; Van Oost, K.; Vogel, C.; Boeckx, P., Links among warming, carbon and microbial dynamics mediated by soil mineral weathering. *Nat. Geosci.* **2018,** *11* (8), 589-593.
(36) Jahn. R; K, S., Development of soils and site qualities on basic volcanoclastics with special reference to the semiarid environment of lanzarote, canary islands, spain. *Rev. Mex. Cienc. Geol.* **1996,** *13* (1), 8.
(37) Schlesinger, W. H., Evidence from chronosequence studies for a low carbon-storage potential of soils. *Nature* **1990,** *348* (6298), 232-234.
(38) Davis, J. A., Adsorption of natural dissolved organic matter at the oxide/water interface. *Geochim. Cosmochim. Acta* **1982,** *46* (11), 2381-2393.
(39) Pommerenk, P.; Schafran, G. C., Adsorption of inorganic and organic ligands onto hydrous aluminum oxide: Evaluation of surface charge and the impacts on particle and nom removal during water treatment. *Environ. Sci. Technol.* **2005,** *39* (17), 6429-6434.
(40) Saito, T.; Koopal, L. K.; van Riemsdijk, W. H.; Nagasaki, S.; Tanaka, S., Adsorption of humic acid on goethite: Isotherms, charge adjustments, and potential profiles. *Langmuir* **2004,** *20* (3), 689-700.
(41) Tipping, E., Some aspects of the interactions between particulate oxides and aquatic humic substances. *Mar. Chem.* **1986,** *18* (2), 161-169.
(42) Au, K.-K.; Penisson, A. C.; Yang, S.; O'Melia, C. R., Natural organic matter at oxide/water interfaces: Complexation and conformation. *Geochim. Cosmochim. Acta* **1999,** *63* (19), 2903-2917.
(43) Moore, T. R.; de Souza, W.; Koprivnjak, J. F., Controls on the sorption of dissolved organic carbon by soils. *Soil Sci.* **1992,** *154* (2).
(44) Schrumpf, M.; Kaiser, K.; Guggenberger, G.; Persson, T.; Kögel-Knabner, I.; Schulze, E. D., Storage and stability of organic carbon in soils as related to depth, occlusion within aggregates, and attachment to minerals. *Biogeosciences* **2013,** *10* (3), 1675-1691.
(45) Avneri-Katz, S.; Young, R. B.; McKenna, A. M.; Chen, H.; Corilo, Y. E.; Polubesova, T.; Borch, T.; Chefetz, B., Adsorptive fractionation of dissolved organic matter (dom) by mineral soil: Macroscale approach and molecular insight. *Organic Geochemistry* **2017,** *103*, 113-124.

(46) Kleber, M.; Bourg, I. C.; Coward, E. K.; Hansel, C. M.; Nunan, N., Dynamic interactions at the mineral–organic matter interface. *Nat. Rev. Earth & Environ.* **2021**, *2*, 402-421.
(47) Kögel-Knabner, I., The macromolecular organic composition of plant and microbial residues as inputs to soil organic matter. *Soil Biol. Biochem.* **2002,** *34* (2), 139-162.
(48) Gallet, C.; Pellissier, F., Phenolic compounds in natural solutions of a coniferous forest. *J. Chem. Ecol.* **1997,** *23* (10), 2401-2412.
(49) Zech, W.; Guggenberger, G.; Schulten, H.-R., Budgets and chemistry of dissolved organic carbon in forest soils: Effects of anthropogenic soil acidification. *Sci. Total Environ.* **1994,** *152* (1), 49-62.
(50) Chorover, J.; Amistadi, M. K., Reaction of forest floor organic matter at goethite, birnessite and smectite surfaces. *Geochim. Cosmochim. Acta* **2001,** *65* (1), 95-109.
(51) Leinemann, T.; Preusser, S.; Mikutta, R.; Kalbitz, K.; Cerli, C.; Höschen, C.; Mueller, C. W.; Kandeler, E.; Guggenberger, G., Multiple exchange processes on mineral surfaces control the transport of dissolved organic matter through soil profiles. *Soil Biol. Biochem.* **2018,** *118*, 79-90.
(52) Keiluweit, M.; Kleber, M., Molecular-level interactions in soils and sediments: The role of aromatic π-systems. *Environ. Sci. Technol.* **2009,** *43* (10), 3421-3429.
(53) Kunhi Mouvenchery, Y.; Kučerík, J.; Diehl, D.; Schaumann, G. E., Cation-mediated cross-linking in natural organic matter: A review. *Rev. Environ. Sci. Biotechnol.* **2012,** *11* (1), 41-54.
(54) Percival, H. J.; Parfitt, R. L.; Scott, N. A., Factors controlling soil carbon levels in new zealand grasslands is clay content important? *Soil Sci. Soc. Am. J.* **2000,** *64* (5), 1623-1630.
(55) Koestel, J.; Schlüter, S., Quantification of the structure evolution in a garden soil over the course of two years. *Geoderma* **2019,** *338*, 597-609.
(56) Lajtha, K.; Crow, S. E.; Yano, Y.; Kaushal, S. S.; Sulzman, E.; Sollins, P.; Spears, J. D. H., Detrital controls on soil solution n and dissolved organic matter in soils: A field experiment. *Biogeochemistry* **2005,** *76* (2), 261-281.
(57) Zieger, A.; Kaiser, K.; Ríos Guayasamín, P.; Kaupenjohann, M., Massive carbon addition to an organic-rich andosol increased the subsoil but not the topsoil carbon stock. *Biogeosciences* **2018,** *15* (9), 2743-2760.
(58) Lal, R., Digging deeper: A holistic perspective of factors affecting soil organic carbon sequestration in agroecosystems. *Global Change Biol.* **2018,** *24* (8), 3285-3301.